Japanese Journal of Applied Physics, Vol. 46, No. 24, 2007, pp. L590-L592

# Chemical and Potential-Bending Characteristics of $SiN_x$/AlGaN Interfaces Prepared by *In Situ* Metal-Organic Chemical Vapor Deposition

Eri Ogawa*, Tamotsu Hashizume, Satoshi Nakazawa[1], Tetsuzo Ueda[1] and Tsuyoshi Tanaka[1]

Research Center for Integrated Quantum Electronics (RCIQE) and Graduate School of Information Science and Technology, Hokkaido University,
[1]Semiconductor Devices Research Center, Matsushita Electric Industrial Company
Takatsuki, Osaka 569-1193, Japa Sapporo 060-8628, Japan n

We investigate the chemical and potential-bending characteristics of *in situ* $SiN_x$/AlGaN interfaces prepared by metal-organic chemical vapor deposition. X-ray photoelectron spectroscopy showed that the *in situ* $SiN_x$ layer had typical chemical binding energies corresponding to the Si-N bonds. The *in situ* $SiN_x$ deposition brought no chemical degradation on the AlGaN surface at the $SiN_x$/AlGaN interface, whereas the *ex situ* deposition of $SiN_x$ by a plasma process induced chemical disorder on the AlGaN surface including a composition change and the formation of interfacial oxides. A significant reduction in the surface band bending was observed on the AlGaN surface after the *in situ* $SiN_x$ passivation, probably due to a decrease in the surface state density.

KEYWORDS: SiN, *in situ*, MOCVD, AlGaN, XPS, surface, potential
* e-mail : ogawa@rciqe.hokudai.ac.jp

Surface passivation structures using dielectric films such as $SiO_2$, $SiN_x$, AlN, and $Al_2O_3$ among others, are very important for the realization of operation stability and reliability for various kinds of semiconductor devices. For GaN field-effect transistors (FETs), in particular, it has been reported that the $SiN_x$-based passivation scheme is effective in suppressing "current collapse effects" [1-3] due to a relatively low state density at the $SiN_x$/AlGaN interface.[4-6] Very recently, Derluyn *et al.*[7] have reported that the *in situ* deposition of $SiN_x$ on the AlGaN surface significantly improved the DC performance of AlGaN/GaN high-electron mobility transistors (HEMTs). However, the physical mechanism of its passivation effects on the HEMT characteristics is not yet known. In this paper, we investigate the chemical and potential-bending characteristics of the *in situ* $SiN_x$/AlGaN interfaces prepared by metal-organic chemical vapor deposition (MOCVD).

**Figure 1** shows the sample structures. We grew undoped $Al_{0.4}Ga_{0.6}N$/undoped GaN structures on sapphire substrates by MOCVD. *In situ* deposition of an ultrathin $SiN_x$ layer (~ 1 nm) was carried out at 1000 °C, as shown in Fig. 1(a), using $SiH_4$ and $NH_3$ as precursors for Si and N atoms, respectively. For comparison, we prepared a reference structure having an *ex situ*-deposited $SiN_x$ layer, as shown in Fig. 1(b). After the MOCVD growth of the AlGaN/GaN heterostructures, the samples were transferred to a plasma-enhanced chemical vapor deposition (PECVD) chamber through air. Then, a $SiN_x$ layer with a thickness of 3 nm was deposited on the AlGaN surface at 300 °C, using $SiH_4$ and $NH_3$. The chemical properties of the $SiN_x$ layers and $SiN_x$/AlGaN interfaces were characterized using an X-ray photoelectron spectroscopy (XPS) system (Perkin-Elmer PHI 1600C) equipped with a spherical capacitor analyzer and a monochromated Al $K\alpha$ radiation source ($h\nu$ = 1486.6 eV).

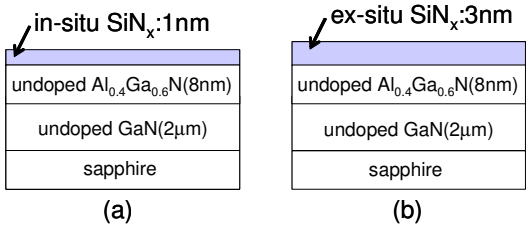


Fig. 1. Sample structures with (a) *in situ* and (b) *ex situ* $SiN_x$ passivation layers.

**Figure 2** shows the Si2*p* and N1*s* core-level spectra with an electron escape angle of 15° obtained from the *in situ* $SiN_x$ surface. Because of the ultrathin thickness of the $SiN_x$ layer, the Ga3*p* signal from AlGaN underneath was overlapped with the Si2*p* line, whereas the N1*s* spectra included other N1*s* and Ga Auger signals from the AlGaN bond, even when using a very shallow detection angle. Thus, we deconvoluted both spectra using a combination of Gaussian and Lorentzian functions. The solid lines in Fig. 2 indicate the deconvoluted spectra. We found that the energy positions were 102.2 and 397.8 eV for the Si2*p* and N1*s* levels, respectively. These energies are very similar to those of the binding energies for

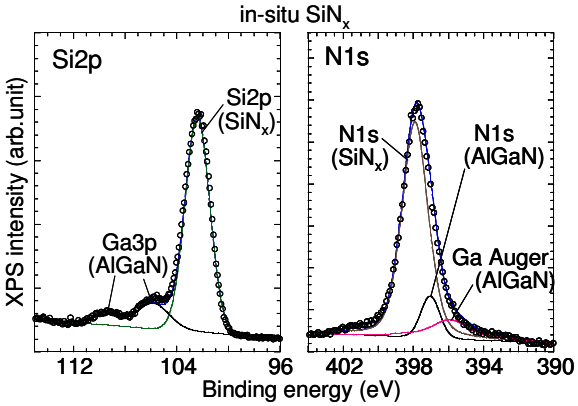


Fig.2 XPS Si2*p* and N1*s* spectra from the *in situ* $SiN_x$ layer deposited on AlGaN/GaN heterostructure.

the Si-N bond.[8] The N composition of the *in situ* $SiN_x$ film, estimated from the integrated XPS intensities of the Si2*p* and N1*s* core levels, was 1.25, indicating a slightly Si-rich film in reference to a standard $Si_3N_4$ composition.

Since the expected thickness of the $SiN_x$ film is only 1 nm, we checked whether the *in situ*-deposited $SiN_x$ had a layer structure or an island structure by angle-resolved XPS. If the sample has a layer structure, as shown in Fig. 3(a), the intensity ratio of Si2*p* to Ga3*p* is given by the following equation:[9]

$$\frac{I_{Si2p}}{I_{Ga3p}} = \frac{S_{Si2p}}{S_{Ga3p}}\left[\exp\left(\frac{d}{\lambda \sin\theta}\right) - 1\right] \qquad (1),$$

where $S_{Si2p}$ and $S_{Ga3p}$ are the XPS sensitivity factors for the Si2*p* and Ga3*p* core levels, respectively, d is the thickness of the $SiN_x$ layer, λ is the electron escape depth in an inelastic collision process, and θ is the electron escape angle. Since the electron kinetic energies from the Si2*p* and Ga3*p* levels are about 1400 eV, we used λ= 2.0 nm for the calculation.[10] Figure 3(b) shows the experimental and calculated ratios as a function of the escape angle. The angle dependence of the Si2*p* and Ga3*p* spectra is shown in the inset of Fig. 3(b). The measured ratio was in excellent agreement with the calculated curve, indicating that the *in situ* deposited $SiN_x$ film has a layer structure with high uniformity. The best fitting result allowed d = 1.2 ± 0.2 nm, which is very similar to that expected by the deposition rate. For the PECVD $SiN_x$ film, the thickness was estimated to be 2.5 ± 0.3 nm.

**Figure 4** shows the Al2*p* and Ga3*d* core-level spectra of the AlGaN surfaces with the $SiN_x$ layers prepared by *in situ* and *ex situ* processes. For the *in situ* sample, both the Al2*p* and Ga3*d* spectra were represented by each single component arising from the Al-N bond and Ga-N bond, respectively, in the AlGaN lattice. From the integrated XPS intensity, we found an Al composition of 39 %, which is very similar to the expected value by the growth condition.

Thus, the *in situ* deposition of $SiN_x$ brought no significant effects on the chemical bonding state of the as-grown AlGaN surface. On the other hand, the *ex situ* sample showed oxide-related peaks in the Al2*p* and the Ga3*d* spectra, as shown in Fig. 4. After the growth of the AlGaN/GaN layer structure, the AlGaN surface was exposed to air, resulting in the formation of natural oxide consisting of $Ga_2O_3$ and $Al_2O_3$ on the AlGaN surface.[5,11] In particular, the formation of Al oxide was more enhanced than that of Ga oxide, due to the highly reactive property of Al with oxygen, probably causing a composition change on the AlGaN surface. Even after the PECVD of $SiN_x$, such chemical degradation, including the composition change and the formation of interfacial oxides, remained on the AlGaN surface.

Finally, we estimated surface potential on the AlGaN surface from the core-level energy and the valence band edge. We plotted the Ga3*d* spectra of the $SiN_x$/AlGaN samples and bare AlGaN surface exposed to air in Fig. 5(a). In comparison to the peak position of the air-exposed sample, a slight shift toward higher energies was observed in the Ga3*d* peak of the *ex situ* $SiN_x$/AlGaN sample. In the *in situ* sample, we observed a large peak shift of about 0.6 eV, as shown in Fig. 5(a). Similar peak-energy shifts were confirmed in the Al2*p* and N1*s* core levels. Then, we estimated the energy position of the valence band (VB) maximum from the onset of the VB spectra, as shown in Fig. 5(b). The air-exposed AlGaN surface exhibited a VB maximum energy of 2.6 eV from the Fermi level, $E_F$. A higher onset energy of 0.6 eV was obtained for the *in situ* $SiN_x$/AlGaN sample. Such

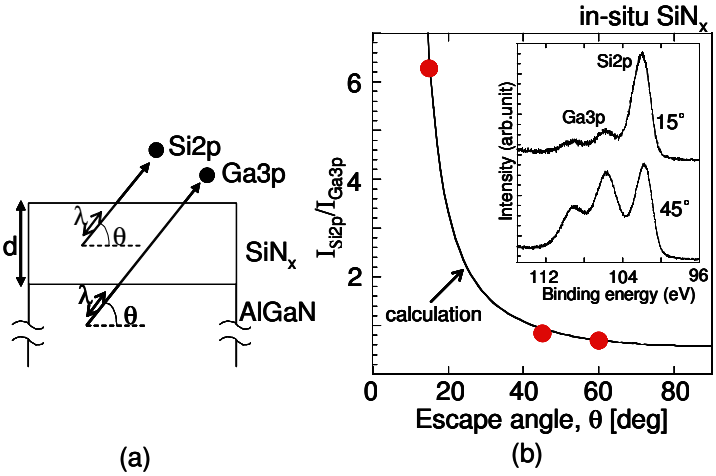


Fig.3 (a) Schematic illustration of photoelectron emission process from the $SiN_x$/AlGaN layer structure. (b) XPS intensity ratio of Si2*p* to Ga3*p* as a function of electron escape angle. The solid line indicates the calculated ratio using d= 1.2 nm and λ= 2.0 nm. The inset shows the angle dependence of the XPS spectra.

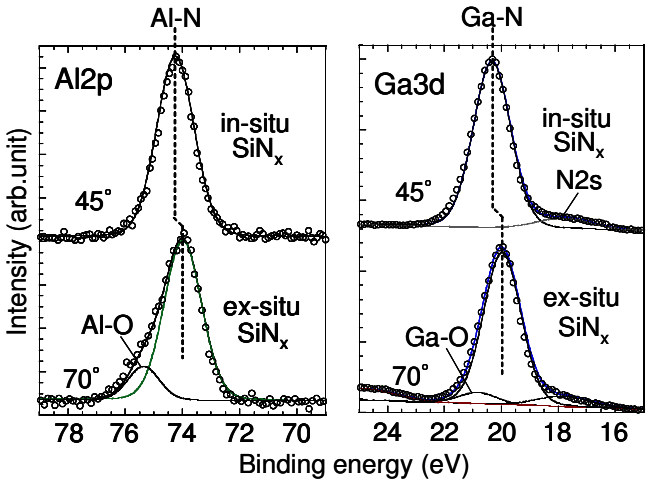


Fig.4 Al2*p* and Ga3*d* spectra for the $SiN_x$/AlGaN interfaces.

difference in the onset energy was consistent with the energy difference in the Ga3*d* peaks. Note that such analysis was impossible on the VB spectrum for the *ex situ* $SiN_x$/AlGaN sample, because a thicker $SiN_x$ layer significantly impeded the appearance of the AlGaN VB spectrum.

From the energy difference in the VB onset or the Ga3*d* peak, the surface potential (surface band bending) on the AlGaN surface was estimated for the air-exposed and the $SiN_x$-passivated samples. We defined the surface potential, $E_S$, on the AlGaN surfaces as follows:

$$E_S = E_C - E_F = E_G - (E_F - E_V) \quad (2),$$

where $E_C$ is the energy at the conduction band minimum, $E_g$ is the bandgap of $Al_xGa_{1-x}N$ ($E_G$ =4.2 eV for x=0.4), and $E_V$ is the energy at the valence band maximum. The estimated $E_S$ values of the air-exposed and $SiN_x$-passivated AlGaN surfaces are plotted in Fig. 6. Only for the *ex situ* $SiN_x$/AlGaN sample, $E_S$ was determined from the Ga3*d* peak energy relative to that of the air-exposed sample, as mentioned above.

We obtained an $E_S$ of 1.6 eV on the air-exposed AlGaN surface. $E_S$ values ranging from 1.3 to 1.7 eV have often been reported for $Al_xGa_{1-x}N$ surfaces (x: 0.24–0.41).[6, 12-14] Originating from the termination of crystalline periodicity, the composition change, and the formation of an interfacial transition layer on the semiconductor surfaces, the separation of the density of states into the conduction and valence bands becomes insufficient at the insulator-semiconductor interfaces, generally inducing the so-called interface states. This suggests that the upper half of the state continuum has a conduction-band character with an acceptor-like charging nature, whereas the lower-half one is derived from the valence-band states with a donor-like charging nature.[15]

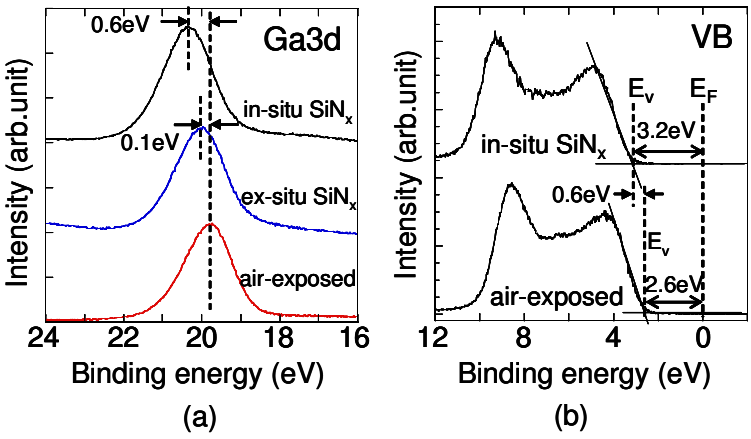


Fig.5 (a) Ga3*d* spectra for the air-exposed AlGaN surface and the $SiN_x$/AlGaN interfaces. (b) Valence band spectra for the air-exposed and *in situ* $SiN_x$ passivated AlGaN surfaces.

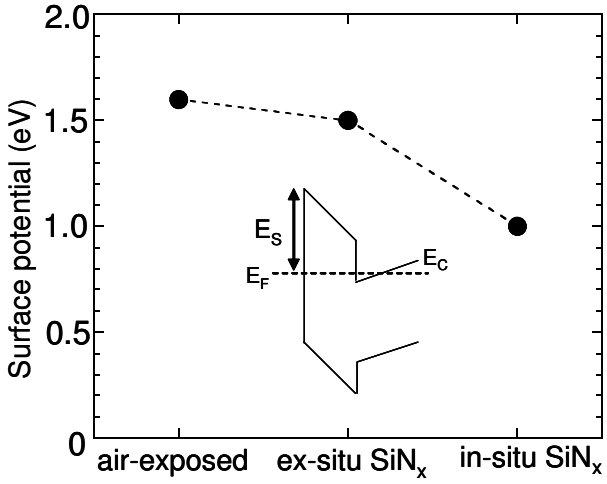


Fig.6 Surface potential values for the air-exposed and the $SiN_x$ passivated AlGaN surfaces.

The branching point between the two kinds of state continuum can act as a charge neutrality level.[16] It is likely that the air-exposed AlGaN surface has high-density interface states due to chemical degradation as mentioned above. The acceptor-like states occupied with electrons can induce a large amount of negative charge on the AlGaN surface, thereby increasing the surface potential of AlGaN. The surface passivation structure utilizing the *ex situ* deposition of $SiN_x$ may slightly reduce the surface states. After the *in situ* $SiN_x$ passivation, we observed a pronounced reduction in surface potential down to 1.0 eV, as shown in Fig. 6. As shown in Fig. 4, no chemical degradation was brought on the AlGaN surface after the *in situ* deposition of $SiN_x$. The *in situ* CVD provided no interfacial composites such as oxides and less processing energy to the AlGaN surface than the plasma-assisted process. Thus, the surface passivation structure having *in situ*-deposited $SiN_x$ could be effective in reducing the electronic states on the AlGaN surface.

There remains a possibility that the difference in the passivation effect between the *in situ* and *ex situ* $SiN_x$ layers comes from the difference in their insulating film quality. The *ex situ* $SiN_x$ layer was deposited at a relatively low temperature (300 $^oC$). In this case, the film usually includes many H atoms and becomes coarse. In comparison with the *in situ* $SiN_x$ layer deposited at 1000 $^oC$, such an inferior film quality of the *ex situ* $SiN_x$ can cause a reduction in its bandgap and/or a change in its band alignment to AlGaN, affecting the surface potential of the AlGaN surface at the $SiN_x$/AlGaN interface. Thus, further investigation is needed to obtain better insight into the passivation effects of the $SiN_x$ deposition on the AlGaN surface.

In summary, we investigated the chemical and potential-bending characteristics of $SiN_x$/AlGaN interfaces. By

angle-resolved XPS, we confirmed that *in situ* $SiN_x$ had a layer structure with a thickness of 1.2 nm. The *in situ* $SiN_x$ deposition brought no degradation on the chemical bonding states of the AlGaN surface, whereas the *ex situ* deposition of $SiN_x$ by a plasma process induced chemical degradation on the AlGaN surface including a composition change and the formation of interfacial oxides. In addition, the *in situ* deposition of $SiN_x$ resulted in a significant reduction in surface potential bending on the AlGaN surface, probably due to a decrease in the surface state density. A surface passivation structure utilizing an *in situ* $SiN_x$ layer can be promising for improving the stability and reliability of GaN-based devices.


1) B. M. Green, K. K. Chu, E.M. Chumbes, J.A. Smart, J.M. Shealy and L.F. Eastman: IEEE Electron Device Lett. **21** (2000) 268.
2) Y. Okamoto, Y. Ando, T. Nakayama, Koji Hataya, H. Miyamoto, T. Inoue, M. Senda, K. Hirata, M. Kosaki, N. Shibata, and M. Kuzuhara: IEEE Trans. Electron Devices, **51** (2004) 2217.
3) T. Kikkawa: Jpn. J. Appl. Phys. **44** (2005) 4896.
4) T. Hashizume, S. Ootomo, S. Oyama, M. Konishi and H. Hasegawa: J. Vac. Sci. Technol. B **19** (2001) 1675.
5) T. Hashizume, S. Ootomo, T. Inagaki and H. Hasegawa: J. Vac. Sci. Technol. B **21** (2003) 1828.
6) T. Hashizume and H. Hasegawa: Appl. Surf. Sci. **234** (2004) 387.
7) J. Derluyna, S. Boeykens, K. Cheng, R. Vandersmissen, J. Das, W. Ruythooren, S. Degroote, M. R. Leys, M. Germain, and G. Borghs: J. Appl. Phys. **98** (2005) 054501.
8) R. Kaercher, L. Lay, and R.L. Johnson: Phys. Rev. B **30** (1984) 1896.
9) S. Hofman and J. M. Sanz: Surf. Interface Anal. **6** (1984) 75.
10) D. R. Penn: Phys. Rev. B **35** (1987) 482.
11) T. Hashizume, S. Ootomo, R. Nakasaki, S. Oyama, M. Kihara: Appl. Phys. Lett. **76** (2000) 2880.
12) H.W. Jiang, C.M. Jeon, K.H. Kim, J.K. Kim, S.B. Bae, J.H. Lee, J.W. Choi, J.L. Lee: Appl. Phys. Lett. **81** (2002)1249.
13) A. Rizzi, H. Luth: Appl. Phys. A **75** (2002) 69.
14) S. Heikman, S. Keller, Y. Wu, J.S. Speck, S.P. DenBaars, K. Mishra: J. Appl. Phys. **93** (2003) 10114.
15) H. Lueth: *Surfaces and Interfaces of Solids*, (Splinger-Verlag, Berlin, 1993) 2nd. Ed., Chapter 6.
16) W. Moench, Appl. Sur. Sci. **117/118** (1997) 380.